 

DOI: 10.1070/QEL16188

# Control over the resonance wavelength of fibre Bragg gratings using resistive coatings based on single-wall carbon nanotubes

Yu.G. Gladush, O.I. Medvedkov, S.A. Vasil'ev, D.S. Kopylova, V.Ya. Yakovlev, A.G. Nasibulin

*Abstract.* **We demonstrate that a thin resistive coating based on single-wall carbon nanotubes applied to the lateral surface of an optical fibre allows it to be uniformly heated up to a temperature of ~400 °C without damage to the coating. Using a fibre Bragg grating (FBG) as an example, we assess the efficiency of resonance wavelength thermal tuning and examine frequency characteristics that can be achieved using such coating. In particular, we show that the resonance wavelength of the FBG can be tuned over 3.2 nm with an efficiency of 8.7 nm $W^{-1}$ and time constant of ~0.4 s.**

***Keywords:*** *optical fibre, fibre Bragg gratings, single-wall carbon nanotubes.*

## 1. Introduction

Fibre Bragg gratings (FBGs) are used successfully in many optical and optoelectronic applications. Possessing unique spectral characteristics, such gratings are used as mirrors of fibre laser cavities and optical converters, to stabilise the wavelength of semiconductor lasers [1], as narrow-band filters and dispersion compensators in optical fibre communication systems [2], as sensing elements of fibre-optic sensors for a variety of applications [3] and for other purposes.

The resonance wavelength of an FBG written into a single-mode fibre is determined by the phase matching condition $\lambda_{BG} = 2n_{eff}\Lambda$ (where $n_{eff}$ is the effective refractive index of the fundamental mode of the fibre and $\Lambda$ is the FBG period). Controlled precision tuning of the resonance wavelength of an FBG, necessary for the ability to tune the frequency of laser sources, as well as in fibre-optic sensors, optical modulators, switches and gates, is typically ensured by longitudinal deformation of the FBG-containing fibre section [4] or by varying its temperature [5]. In the case of fibre deformation, the change in $\lambda_{BG}$ is mostly due to the change in grating period $\Lambda$, whereas the temperature influences primarily $n_{eff}$ [6]. Longitudinal fibre deformation allowed $\lambda_{BG}$ to be tuned over several tens of nanometres in ~1 ms, without significant changes in the shape of the FBG spectrum [4]. If an FBG is heated by thin-film resistive coatings, the resonance wavelength tuning range is narrower, but the fibre is not subject to deformation and there is no need to firmly secure it in a deformation system. In particular, Limberger et al. [5] demonstrated a $\lambda_{BG}$ shift by 2.15 nm with an efficiency of 4.1 nm $W^{-1}$ as a result of resistive heating of a silica fibre coated with a thin platinum layer. High tuning efficiency (13.4 nm $W^{-1}$) was achieved by using optical fibre based on polymethyl methacrylate (PMMA), whose refractive index is a stronger function of temperature [7].

At present, films based on single-wall carbon nanotubes (SWCNTs) applied to the fibre end face are widely used as saturable absorbers to control parameters of fibre lasers [8]. An SWCNT-based coating applied to the lateral surface of a long-period fibre grating (LPFG) makes it possible to substantially improve the sensitivity of the resonance wavelength of such gratings to changes in the refractive index of the ambient medium [9].

In this paper, we examine the feasibility of tuning the resonance wavelength of an FBG via the resistive heating of an SWCNT-based film produced on the lateral surface of fibre in the FBG region.

## 2. Experimental samples and measuring equipment

Fibre Bragg gratings were UV written into an SMF-28e standard telecom fibre by a frequency-doubled $Ar^+$ laser (244 nm) using a Lloyd interferometer-based writing system [10]. To improve the photosensitivity of the fibre, it was first subjected to low-temperature hydrogen loading in a chamber at a pressure of ~100 atm and temperature of 90 °C for 20 h. The molecular hydrogen remaining in the glass network after FBG inscription was removed by similar heat treatment.

The resonance wavelength of the FBGs was near 1.55 μm. The gratings (~4 mm in length) had high reflectivity (~99%) and a bandwidth (FWHM) of ~0.5 nm.

Before FBG inscription, an ~10-mm-long section of the fibre was mechanically stripped of the protective polymer coating. After grating inscription, a coating consisting of several tens of SWCNT-containing layers was produced on this section. Carbon nanotubes for the coating were synthesised by aerosol chemical vapour deposition: thermal decomposition of ferrocene [$Fe(C_5H_5)_2$] vapour in a carbon monoxide (CO) atmosphere [11]. The SWCNTs thus prepared were col-

**Yu.G. Gladush** Institute of Spectroscopy, Russian Academy of Sciences, Fizicheskaya ul. 5, Troitsk, 142190 Moscow, Russia; e-mail: Y.Gladush@skoltech.ru;
**O.I. Medvedkov, S.A. Vasil'ev** Fiber Optics Research Center, Russian Academy of Sciences, ul. Vavilova 38, 119333 Moscow, Russia; e-mail: medoi@fo.gpi.ru;
**D.S. Kopylova, V.Ya. Yakovlev** Skolkovo Institute of Science and Technology, ul. Nobelya 3, 143026 Moscow, Russia;
**A.G. Nasibulin** Skolkovo Institute of Science and Technology, ul. Nobelya 3, 143026 Moscow, Russia; Peter the Great St. Petersburg Polytechnic University, Politekhnicheskaya ul. 29, 195251 St. Petersburg, Russia; Department of Applied Physics, School of Science, Aalto University, P.O. Box 15100, FI-00076, Espoo, Finland

Received 28 July 2016; revision received 17 September 2016
*Kvantovaya Elektronika* **46** (10) 919–923 (2016)
Translated by O.M. Tsarev

lected on a cellulose filter placed at the reactor outlet [12, 13]. The thickness of the films formed on the filter surface and containing randomly arranged SWCNTs was determined by the collection time and was ~40 nm in our experiments (this value was obtained by analysing the transmission of the films at a wavelength of 550 nm [14]). The as-prepared films had high electrical conductivity, which was insensitive to bending and stretching. This is essential for film application to a bent surface. The films were transferred from the filter surface to the lateral surface of the stripped fibre section containing the FBG as follows: the film on the filter was pressed against the fibre and stuck to it. Next, it was wound onto the fibre (40–50 turns).

To improve the conductive properties of the coating, the coated fibre section was immersed in a gold chloride (15 mol %) solution in ethanol and held in it for 2 min at a solution temperature of 70 °C [15, 16]. Owing to this doping procedure, the electrical resistance of the coating after drying was about ten times lower than its initial resistance, namely 30–40 Ω at a coating length of 15–20 mm (the electrical resistance of the coating is determined by the number of SWCNT layers and gold chloride concentration and may vary from sample to sample).

Figure 1 shows a scanning electron microscopy image of a portion of the lateral fibre surface coated with SWCNTs. Analysis of such images showed that the coating was highly uniform along the fibre axis (there were no folds or other nonuniformities) and that its thickness was ~2.2 μm.

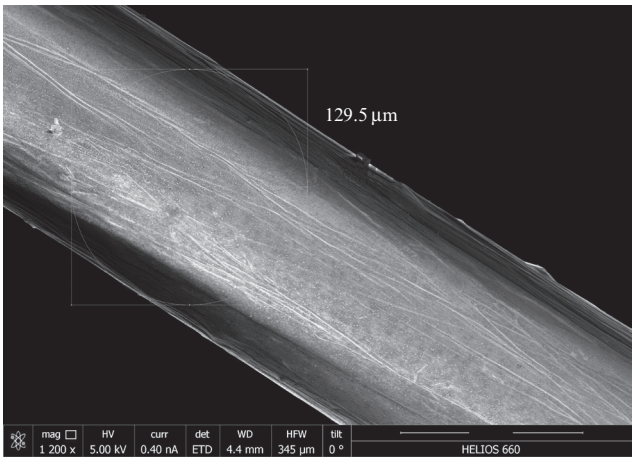


**Figure 1.** Scanning electron microscopy image of an optical fibre coated with a SWCNT-based film.

The electrical resistance of the coating was measured as a function of its length by the four probe method using an MPI TS150 probe station and Keysight 34410A multimeter, and the results confirmed that the coating was spatially uniform. As seen in Fig. 2, the experimental data are well represented by the best fit straight line with a slope of 1.3 Ω mm$^{-1}$.

Electrodes were secured to the SWCNT coating surface by CW2400 conductive epoxy. To ensure a better temperature distribution uniformity in the FBG-containing fibre section, the electrodes were located about 5 mm away from the grating edges.

For steady-state heating of the coating, we used a Tektronix PWS4305 dc power supply, and an alternating current was provided by a Tektronix AFG3101C arbitrary function generator. The reflection and transmission spectra of the FBGs were measured using a superluminescent erbium-doped fibre source and an ANDO-6317B spectrum analyser with a spectral resolution of 0.01 nm. To study transient processes, we used an FIU-44-1.55-40-Er FBG interrogation unified recording module, which allowed us to measure the FBG resonance wavelength at a frequency of 1 kHz with an accuracy of 1 pm or better. The measurements were performed under normal conditions. Note that the fibre section in the undeformed state was held by clamps located outside the coating region.

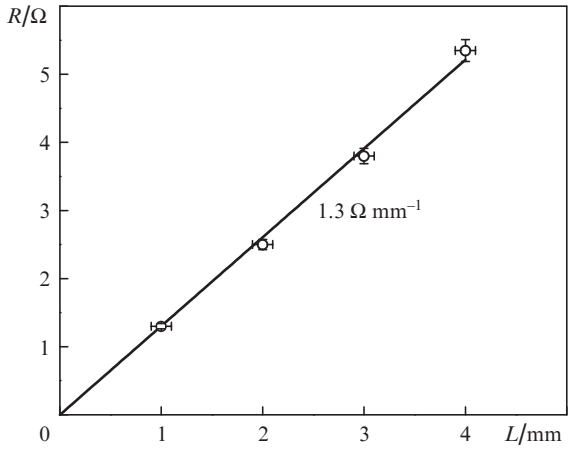


**Figure 2.** Electrical resistance of the coating measured as a function of the separation between the inner contacts by the four probe method.

## 3. Measurement results

The results presented below were obtained for a grating with an SWCNT-based coating $L = 20$ mm in length (contact separation). The room-temperature electrical resistance of the coating was 37 Ω. The FBG-containing fibre section was first heated to a temperature of ~400 °C (using the coating) over a period of several minutes in order to anneal out the least thermally stable component of the photoinduced refractive index in the fibre core, thereby ensuring a constant photoinduced refractive index at lower temperatures [10].

Figure 3a shows transmission spectra of the SWCNT-coated FBG at different applied voltages. It is seen that resistive heating of the coating changes the resonance wavelength of the FBG without significant changes in the shape of the grating spectrum. In our experiments, the reproducible $\lambda_{BG}$ shift reached 3.2 nm at a voltage of 4.5 V. Given that the temperature sensitivity of the FBG resonance wavelength is $d\lambda_{BG}/dT \sim 10$ pm °C$^{-1}$ [6], this shift corresponds to a fibre temperature of ~350 °C. Note that even at this high temperature the shape of the FBG spectrum remained unchanged (Fig. 3a). This indicates not only that the SWCNT coating is homogeneous but also that its properties remain unchanged upon considerable heating. Bending the fibre causes no damage to the coating, nor does it influence heating uniformity.

With increasing temperature, the electrical resistance of the coating increased linearly, with a temperature coefficient of 0.05 Ω K$^{-1}$, as follows from comparison of the voltage and current applied to the coating and the temperature evaluated from the spectral shift of the resonance wavelength, $\Delta\lambda_{BG}$. The temperature dependence of the electrical resistance of SWCNT layers was studied in greater detail elsewhere [17].

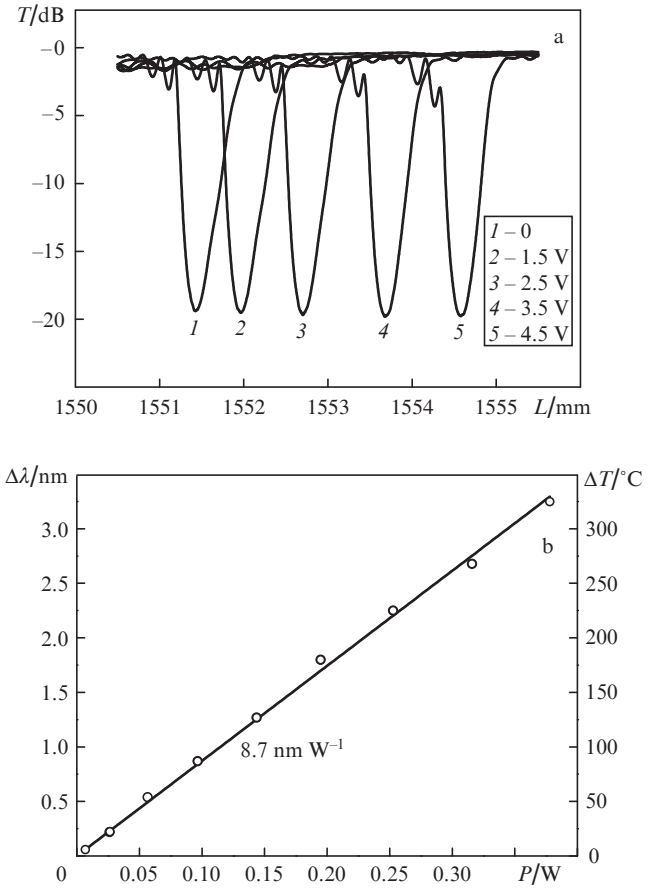


**Figure 3.** (a) Transmission spectra of the FBG at different dc voltages applied to the SWCNT-based coating; (b) effect of the electric power delivered to the coating on the resonance wavelength and temperature of the FBG.

The experimental data in Fig. 3b demonstrate that, in the range under consideration, $\Delta\lambda_{BG}$ is a linear function of the electric power delivered to the coating, with a slope of 8.7 nm $W^{-1}$, which corresponds to a resonance wavelength tuning efficiency $\Delta\lambda_{BG}/P = 4.3$ nm cm $W^{-1}$ for an FBG of unit length. The right-hand vertical axis in Fig. 3b represents the temperature change $\Delta T$ in the SWCNT-coated fibre section as estimated from the temperature sensitivity of $\lambda_{BG}$. It is seen that 0.2 W of electric power is sufficient for heating the fibre to 150 °C. This power correlates with the value reported by Costantini et al. [18] for heating with the use of a resistive metallic coating if we take that the metallic coating was four times longer.

The main mechanism of fibre cooling in our case is convective and radiative heat dissipation through the fibre surface. Heat dissipation is usually quantified using the temperature-independent heat transfer coefficient per unit length, $H$ [19, 20]. The heat balance equation for a fibre section can then be written in the form [19]

$$C\frac{\mathrm{d}(\Delta T)}{\mathrm{d}t} = P(t) - H\Delta T, \tag{1}$$

where $\Delta T$ is the temperature difference between the fibre and ambient medium; $C$ is the heat capacity of a fibre section of unit length (the heat capacity of the coating can be neglected in comparison with that of the fibre); and $P(t)$ is the electric power delivered to the coating per unit coating length. Note that, in the above equation, heat removal through the fibre end faces is usually neglected, but it can be essential at a sufficiently short coating length. Note also that, at a fibre diameter of 125 μm, the time it takes for the radial temperature profile in the fibre to become uniform is rather short (~1 ms), so it is assumed in Eqn (1) that, throughout the fibre, the temperature is the same as in the coating.

Consider the general solution to Eqn (1) for an ac voltage, $V(t) = V_0\sin(\omega t + \varphi/2)$, applied to the coating at $t > 0$, i.e. for the electric power

$$\begin{aligned} P(t) &= 0 \qquad (t \leqslant 0), \\ P(t) &= \frac{P_0}{2}[1 - \cos(2\omega t + \varphi)] \quad (t > 0). \end{aligned} \tag{2}$$

For $t > 0$, the solution has the form

$$\Delta T(t) = \frac{P_0}{2H}\left\{1 - \frac{4\omega^2\tau^2}{1 + 4\omega^2\tau^2}\exp(-t/\tau) - \frac{1}{\sqrt{1 + 4\omega^2\tau^2}}\cos[2\omega t + \varphi - \arctan(2\omega\tau)]\right\}, \tag{3}$$

where $\tau = C/H$ is the time constant for the heating and cooling of the coated fibre section.

The above $P(t)$ dependence set by us allows simple solutions for the fibre heating profiles considered below to be found from (3). In particular, a solution for steady-state heating of the coating follows from (3) at $\omega = 0$ and $\varphi = \pi$:

$$\Delta T = P_0/H. \tag{4}$$

Thus, in the case of steady-state heating, the temperature of the fibre is a linear function of the electric power delivered to it, which is well consistent with the data presented in Fig. 3b. The heat transfer coefficient $H$ of the surface of the SWCNT-coated fibre is 0.05 W $K^{-1}$ $m^{-1}$ as evaluated from the slope of the line in Fig. 3b. This value coincides with that obtained by Costantini et al. [18] for a metal-coated fibre.

In the case of a sharp change in heating power (an increase in power from 0 to $P_0/2$), solution (3) for $\omega \to \infty$ takes the form

$$\Delta T(t) = \frac{P_0}{2H}[1 - \exp(-t/\tau)]. \tag{5}$$

The time constant $\tau$ was measured by applying a rectangular voltage pulse of 15 s duration and 0.6 V amplitude to the coating. The time dependence of $\Delta\lambda_{BG}$ thus obtained is presented in Fig. 4. The leading and trailing edges of the curve are well represented by exponentials of the form $1-\exp(-t/\tau)$ with $\tau = 0.46$ s in both cases, which agrees well with the value obtained by us and that reported by Costantini et al. [18] but exceeds the time constant obtained by White et al. [20] ($\tau$ = 0.25 s).

The frequency characteristic of the FBG response to a harmonic electrical signal is represented by the third term on the right-hand side of (3). The amplitude of the variation in the FBG resonance wavelength is

$$A = \frac{P_0}{2H}\frac{1}{\sqrt{1 + 4\omega^2\tau^2}}\frac{\mathrm{d}\lambda_{BG}}{\mathrm{d}T}. \tag{6}$$

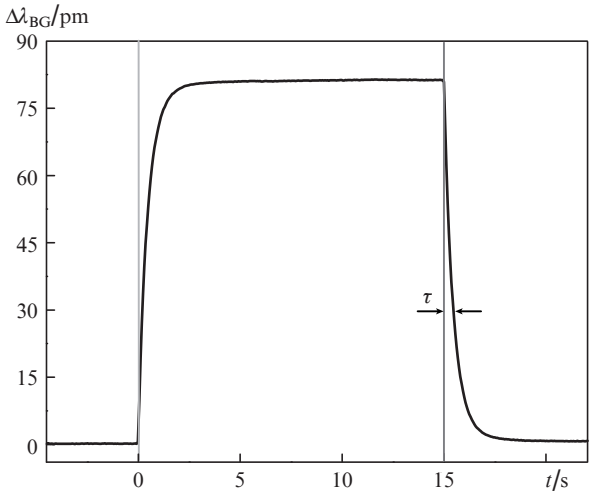


**Figure 4.** Effect of a rectangular voltage pulse on the resonance wavelength of the FBG.

Figure 5a shows the variation in the resonance wavelength of the FBG as the voltage modulation frequency $f = \omega/2\pi$ is increased stepwise in the range 0.01 – 10 Hz at a constant voltage modulation amplitude $V_0 = 3.6$ V. It follows from these data that, at low modulation frequencies ($f \leqslant 0.05$ Hz), the fibre has time enough to reach the temperature corresponding to steady-state heating, whereas at higher frequencies the temperature modulation amplitude and, accordingly, the resonance wavelength of the FBG decrease. As the frequency increases to $f \approx 0.3$ Hz, the modulation amplitude drops by a factor of 2. At a frequency $f \approx 10$ Hz, modulation is essentially indiscernible. Note that the average $\lambda_{BG}$ shift is determined by the average power dissipated in the coating, is independent of the voltage modulation frequency and is half of the steady-state value.

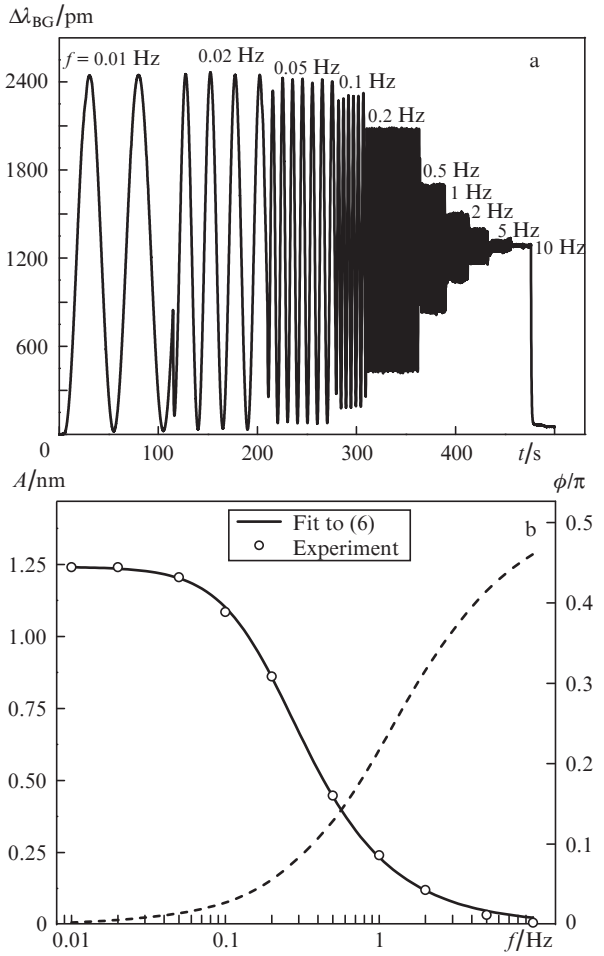


**Figure 5.** (a) Shift of the FBG resonance wavelength at different frequencies of the applied harmonic voltage; (b) $\Delta\lambda_{BG}$ modulation amplitude and phase as functions of frequency.

Figure 4b shows the measured tuning amplitude $A$ (open circles) as a function of modulation frequency $f$. Also presented is a calculated curve obtained by fitting the experimental data with Eqn (6). The best fit was reached at a time constant $\tau = 0.41$ s.

The phase delay of the FBG response to a harmonic electrical signal, $\phi = \arctan(2\omega\tau)$ [see (3)], increases with increasing frequency, approaching $\pi/2$ at high modulation frequencies (Fig. 5b, dashed line).

## 4. Conclusions

We have studied characteristics of a coating based on single-wall carbon nanotubes applied to the lateral surface of an optical fibre via dry transfer. The proposed technique for producing a coating from nanotubes prepared by chemical vapour deposition on a filter has been shown to ensure high uniformity of the electrical and thermal properties of the coating along the length of the fibre and allow the fibre temperature to be tuned over a wide range by resistive heating of the coating. Note that the proposed technique for producing a nanotube coating on the fibre surface is sufficiently simple: it requires no specialized process equipment.

An SWCNT-based coating applied to an FBG-containing fibre section allowed us to tune the resonance wavelength of the grating over more than 3 nm with an efficiency of 8.7 nm $W^{-1}$ by varying the electric power delivered to the coating.

The present results demonstrate that the proposed fibre coating is a viable alternative to resistive metallic coatings and can be used not only to tune the resonance wavelength of FBGs but also to control (stabilise) the phase of a wave in fibre-optic interferometers and phase modulators if the desired phase change time exceeds 100 ms.

***Acknowledgements.*** This work was supported by the RF Ministry of Education and Science (Project No. RFMEFI58114X0006).

## References

1. Archambault J.L., Grubb S.G. *J. Lightwave Technol.*, **15** (8), 1378 (1997).
2. Giles C.R. *J. Lightwave Technol.*, **15** (8), 1391 (1997).
3. Cusano A., Cutolo A., Albert J. (Eds.). *Fiber Bragg Grating Sensors: Recent Advancements, Industrial Applications and Market Exploitation* (Beijing: Bentham Sci. Publ., 2011).
4. Iocco A., Limberger H.G., Salathe R.P., Everall L.A., Chisholm K.E., Williams J.A., Bennion I. *J. Lightwave Technol.*, **17** (7), 1217 (1999).
5. Limberger H.G., Ky N.H., Costantini D.M., Salathé R.P., Muller C.A., Fox G.R. *IEEE Photonics Technol. Lett.*, **10** (3), 361 (1998).
6. Kersey A.D., Davis M.A., Patrick H.J., LeBlanc M., Koo K.P., Askins C.G., Putnam N.A., Friebele E.J. *J. Lightwave Technol.*, **15** (8), 1442 (1997).

7. Kalli K., Dobb H.L., Webb D.J., Carroll K., Komodromos M., Themistos C., Peng G.D., Fang Q., Boyd I.W. *Opt. Lett.*, **32** (3), 214 (2007).
8. Solodyankin M.A., Obraztsova E.D., Lobach A.S., Chernov A.I., Tausenev A.V., Konov V.I., Dianov E.M. *Opt. Lett.*, **33** (12), 1336 (2008).
9. Tan Y.C., Ji W.B., Mamidala V., Chow K.K., Tjin S.C. *Sens. Actuators, B*, **196**, 260 (2014).
10. Vasil'ev S.A., Medvedkov O.I., Korolev I.G., Bozhkov A.S., Kurkov A.S., Dianov E.M. *Kvantovaya Elektron*., **35** (12), 1085 (2005) [*Quantum Electron*., **35** (12), 1085 (2005)].
11. Moisala A., Nasibulin A.G., Brown D.P., Jiang H., Khriachtchev L., Kauppinen E.I. *Chem. Eng. Sci*., **61**, 4393 (2006).
12. Kaskela A., Nasibulin A.G., Zavodchikova M., Aitchison B., Papadimitratos A., Tian Y., Zhu Z., Jiang H., Brown D.P., Zakhidov A., Kauppinen E.I. *Nano Lett*., **10**, 4349 (2010).
13. Nasibulin A.G., Kaskela A.O., Mustonen K., Anisimov A.S., Ruiz V., Kivito S., Rackauskas S., Timmermans M.Y., Pudas M., Aitchison B., Kauppinen M., Brown D.P., Okhotnikov O.G., Kauppinen E.I. *ACS Nano*, **5**, 3214 (2011).
14. Mikheev G.M., Nasibulin A.G., Zonov R.G., Kaskela A., Kauppinen E.I. *Nano Lett*., **12**, 77 (2012).
15. Kim S.M., Kim K.K., Jo Y.W., Park M.H., Chae S.J., Duong D.L., Yang C.W., Kong J., Lee Y.H. *ACS Nano*, **5** (2), 1236 (2011).
16. Gorkina A.L., Tsapenko A.P., Gilshteyn E.P., Koltsova T.S., Larionova T.V., Talyzin A., Anisimov A.S., Anoshkin I.V., Kauppinen E.I., Tolochko O.V., Nasibulin A.G. *Carbon*, **100**, 501 (2016).
17. Kopylova D.S., Boldyrev N.Yu., Yakovlev V.Ya., Gladush Yu.G., Nasibulin A.G. (in press).
18. Costantini D.M., Muller C.A.P., Vasiliev S.A., Limberger H.G., Salathe R.P. *IEEE Photonics Technol. Lett.*, **11** (11), 1458 (1999).
19. Petuchowski S.J., Sigel G.H., Giallorenzi T.G. *Electron. Lett*., **18** (19), 814 (1982).
20. White B., Davis J., Bobb L., Krumboltz H., Larson D. *J. Lightwave Technol*., **5** (9), 1169 (1987).